CHAPTER

4 Live imaging of microtubule dynamics in organotypic hippocampal slice cultures

Philipp Schätzle, Lukas C. Kapitein, Casper C. Hoogenraad[1]

Cell Biology, Faculty of Science, Utrecht University, Utrecht, The Netherlands

[1]*Corresponding author: E-mail: c.hoogenraad@uu.nl*

CHAPTER OUTLINE

Methods in Cell Biology, Volume 131, ISSN 0091-679X, http://dx.doi.org/10.1016/bs.mcb.2015.06.006

Abstract

The microtubule (MT) cytoskeleton plays an active role during different phases of neuronal development and is an essential structure for stable neuronal morphology. MTs determine axon formation, control polarized cargo trafficking, and regulate the dynamics of dendritic spines, the major sites of excitatory synaptic input. Defects in MT function have been linked to various neurological and neurodegenerative diseases and recent studies highlight neuronal MTs as a potential target for therapeutic intervention. Thus, understanding MT dynamics and its regulation is of central importance to study many aspects of neuronal function. The dynamics of MT in neurons can be studied by visualizing fluorescently tagged MT plus-end tracking proteins (+TIPs). Tracking of +TIP trajectories allows analyzing the speeds and directionality of MT growth in axons and dendrites. Numerous labs now use +TIP to track growing MTs in dissociated neuron cultures. This chapter provides detailed methods for live imaging of MT dynamics in organotypic hippocampal slice cultures. We describe protocols for culturing and transducing organotypic slices and imaging MT dynamics by spinning disk confocal microscopy.

INTRODUCTION

Microtubules (MTs) are essential structures for neuronal morphology and synapse function because they serve as tracks for long-distance transport, provide dynamic and mechanical functions, and control local signaling events (Conde & Caceres, 2009; Hirokawa, Niwa, & Tanaka, 2010; Hoogenraad & Bradke, 2009; Maday, Twelvetrees, Moughamian, & Holzbaur, 2014). Axonal transport defects in mature neurons are a common factor in many of the major neurodegenerative diseases, including the motor neuron disease amyotrophic lateral sclerosis and Alzheimer's disease (Encalada & Goldstein, 2014; Millecamps & Julien, 2013). More direct support for the involvement of the MT cytoskeleton in neurodegenerative diseases comes from human genetic studies identifying mutation in various tubulin family members and MT-associated proteins (MAPs) (Breuss & Keays, 2014; Tischfield, Cederquist, Gupta, & Engle, 2011; Zempel & Mandelkow, 2014). MTs have also emerged as a key factor in axonal regrowth potential after spinal cord injury and recent studies highlight MTs as a potential target for therapeutic intervention (Baas & Ahmad, 2013; Bradke, Fawcett, & Spira, 2012; Chisholm, 2013). These studies highlight the importance of MTs for the structure and function of neurons and MT remodeling as a critical mechanism during axon regeneration.

Mature neurons contain a complex array of stable and dynamic MTs, which are differently organized in axons and dendrites. Axonal MTs have a uniform orientation, with their plus-ends oriented towards the axonal tip (plus-end out), whereas dendritic MTs have mixed orientations, with their plus-ends toward either the cell body or the dendritic tip (Baas & Lin, 2011). MT arrays control intracellular transport routes and local signaling pathways and are essential for axon and dendritic functions (Hirokawa et al., 2010; Maday et al., 2014). The organization of MT arrays largely depends on the combined function of different MT regulatory factors or

generally named MAPs. One group of MAPs consists of regulators of MT dynamics, such as plus-end tracking proteins (+TIPs) (Akhmanova & Steinmetz, 2008). The +TIPs either bind directly to the growing MT plus-ends or interact with other plus-end-associated proteins. The dynamic of MTs in living cells can be visualized by time-lapse microscopy using fluorescently tagged +TIPs. The labeled +TIPs appear as comet-shaped signals in microscopic images and can be followed over time in dissociated neuron cultures (Stepanova et al., 2003). For instance, visualizing +TIPs in mature hippocampal neuron cultures has revealed that dynamic MTs are organized in antiparallel arrays and can enter dendritic spines (Jaworski et al., 2009).

Although dissociated neuronal cultures have provided a wealth of information about the basic mechanisms underlying neuronal development and function, organotypic slice cultures can augment these studies and provide experimental conditions that more closely resemble the in vivo situation. Tissue culturing of different rodent species and brain regions has been successfully applied, including hippocampal slice cultures (De Simoni, Griesinger, & Edwards, 2003). The hippocampus is characterized by a laminated structure which contains a trisynaptic circuit connecting the entorhinal cortex with the dentate gyrus, the CA3 and CA1 regions. The specific arrangement of hippocampal neurons, fiber pathways, and specific synaptic connections is preserved in slice cultures. These features, along with the ability to perform experimental manipulations, such as electrophysiological stimulation and drug treatment, make it an excellent experimental model system for studying numerous neurobiological questions. Organotypic cultures have facilitated major breakthroughs in visualizing the dynamics of neuronal morphology and subcellular structures, such as organelles or synaptic protein complexes. Unlike dissociated neuron cultures or acute tissue preparations, cultured slices can be exposed to multiple rounds of imaging sessions, which makes them perfectly suited for studying developmental processes and long-term plasticity in neurons. Particularly, the combination of live cell imaging with local drug applications and/or photostimulation is very strong. For example, the Kasai group has made use of local glutamate uncaging to study actin dynamics in dendritic spines (Honkura, Matsuzaki, Noguchi, Ellis-Davies, & Kasai, 2008). Another interesting example that required spatially restricted activation of individual spines was recently presented by the laboratory of Karen Zito (Oh, Parajuli, & Zito, 2015). Besides the experimental benefits of the conserved tissue organization, an additional strength of slice cultures is its applicability for different forms of high-resolution live imaging. A fascinating example is the analysis of dendritic spines with stimulated emission depletion imaging (Tonnesen, Katona, Rozsa, & Nagerl, 2014). The lateral resolution of about 50 nm allowed the resolution of spine neck properties and demonstrated the impact of spine neck width on the biochemical compartmentalization of the spine head.

In summary, organotypic hippocampal cultures allow application of a great variety of established experimental tools that can be combined with high-resolution imaging of subcellular structures. Here we provide detailed methods for live imaging of MT dynamics in organotypic hippocampal slice cultures. We describe protocols for culturing and transducing organotypic slices and imaging MT dynamic by spinning disk confocal microscopy.

1. EXPRESSION OF MT +TIP MARKERS USING LENTIVIRUS

Ectopic protein expression has been a major challenge in using organotypic slice cultures as an experimental model system. Several viral systems can be used to express proteins in neurons of hippocampal slice cultures (Ehrengruber et al., 2001). Lentiviruses feature a relatively big packaging capacity (~10 kb), as well as the stable integration into the genome of the targeted cell, which we found best suited for our purpose. The integration in the genome has two advantages: first, slices can be infected directly after slice preparation and expression remains stable throughout the culturing period; second, the variable integration sites influence expression of the target constructs which can be useful to find appropriate expression levels for imaging.

The lentivirus is produced by transfecting HEK 293T cells with three different plasmids containing information for packaging (psPAX), viral envelope (p.MDG2), and transfer plasmid with the target expression cassette (pSIN-TRE-S). Viral particles are released to the cell supernatant and can be enriched by tangential flow filtration or ultracentrifugation. The lentivirus is pseudotyped with glycoprotein G from vesicular stomatitis viruses (VSV-G). This envelope allows transduction of postmitotic cells of many cell types and species. However, special care should be given to the virus production conditions because we and others noticed that the viral tropism of VSV-G-pseudotyped virus is shifted towards glial cells when the pH of the culture medium turns acidic due to the high metabolism of the HEK 293T cells during virus production (Torashima, Yamada, Itoh, Yamamoto, & Hirai, 2006).

The lentivirus transfer plasmid is based on the pSIN-TRE-mSEAP-hPGK-rtTA2sM2 third generation vector developed in the Trono lab. This self-inactivating (SIN) vector contains a deletion in the 3′ long terminal repeat (LTR) that is transferred to the 5′ LTR after reverse transcription and leads to a transcriptional inactivation of the LTR in infected cells. As a result the virus is replication incompetent and transduced samples can be transferred to biosafety level I after viral particles have been sufficiently reduced.

The expression of MT +TIP markers is controlled by a tetracycline-inducible expression system. The advantage of this system is the uncoupling of infection time from the start of protein expression. Given the long period between slice infection and image acquisition (>2 weeks), this is essential for obtaining results of high quality. We exchanged the hPGK promotor for the 0.5 kb rat Synapsin promotor (Dittgen et al., 2004), in order to drive neuron specific expression of the tet-transactivator protein (rtTA2sM2). The resulting lentivirus transfer vector was termed pSIN-TRE-S. Following the application of doxycycline, the target proteins are expressed within a few days at sufficient level to perform high-resolution imaging. In our hands, the inducible system outperforms all tested constitutive promotors (CMV, hUBC, EF1-α, Synapsin) in terms of expression levels.

A drawback of the inducible system is a significantly reduced number of transduced cells when comparing the inducible system with the constitutive expressing

promotors in slice cultures or dissociated neurons. Lentiviral encapsidation is a critical step during virus production and it has been shown that vector size strongly influences virus packaging efficiency (Kumar, Keller, Makalou, & Sutton, 2001). The total size of tetracycline response element (0.5 kb), Synapsin promotor (0.5 kb), and tet-transactivator protein (0.75 kb) is however not substantially different from the size of the tested constitutive promotors. Another important step during virus assembly is the amplification of the virion RNA. Transcription mediated by the RSV U3 promotor generates single stranded mRNA that can undergo splicing before its translocation into the virus envelope (Nakagawa et al., 2006). We assume that the TET-inducible cassette makes the transcript more prone to splicing events, which would explain the lower amounts of transduced cells.

In summary, application of lentivirus with an inducible expression system results in transduced neurons with high expression levels, in a sparse pattern throughout the slice culture, which is optimal for high-resolution imaging.

1.1 BUFFERS AND SOLUTIONS

- Complete culture medium: DMEM (Lonza, BE12-604F/U1), 10% FBS, 1% penicillin/streptomycin (Gibco, 15140-122)
- Virus production medium: OptiMEM (Gibco, 31985-047), 1% penicillin/streptomycin
- 1 M HEPES pH 7.4
- 1 mg/mL MAXPEI (Polysciences, 24885)
- Amicon Ultra spin filters (Milipore: UFC910024)

1.2 CLONING GFP-MT+TIP AND MARCKS-TagRFP INTO THE pSIN-TRE-S VECTOR

From the total pool of +TIPs, only a minority is accumulated at the MT plus tip, while the majority remains cytosolic. Accordingly, high expression of fluorescently labeled +TIPs results in a strong diffused background signal which overlays the comet-like signals of dynamic MTs. In our experience, the best signal to noise images is acquired from neurons that exhibit fluorescent signals hardly detectable by eye observation. In order to localize transduced neurons under these conditions, we coexpress a cellular morphology marker along with the MT marker. We solved the need of different expression levels of both markers by cloning a bicistronic construct facilitating strong cap-dependent translation for the cellular morphology marker and weak internal ribosome entry site (IRES)-dependent translation of MT +TIP markers.

1.2.1 MARCKS as a cellular morphology marker

Small neuronal subcompartments like dendritic spines and filopodia contain only low amounts of cytosol and are therefore difficult to resolve by cytosolic localized fluorescent proteins. Instead, we prefer using the N-terminal first 41 amino acids of

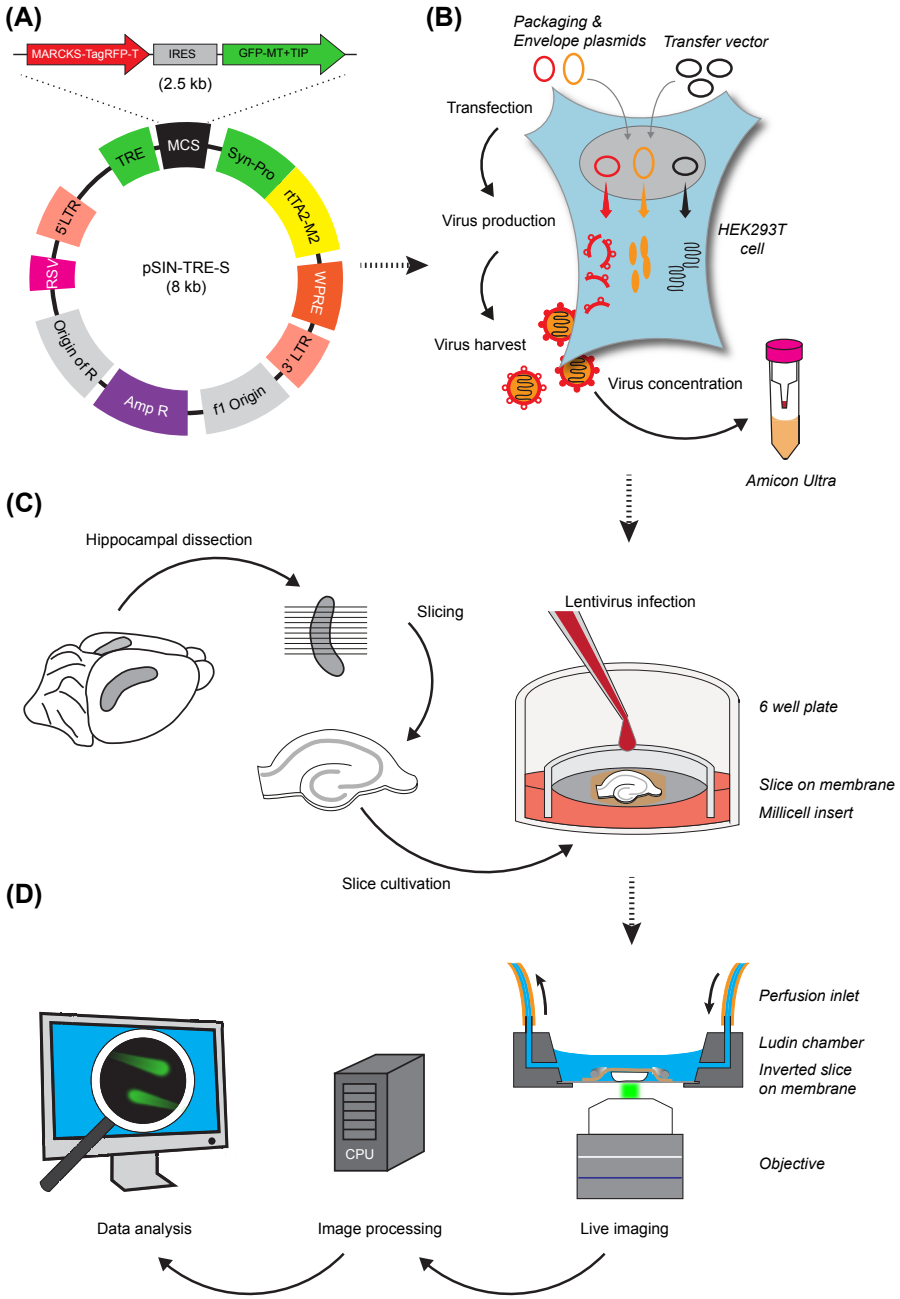

FIGURE 1 Experimental work flow.

(A) Lentivirus transfer vector used for visualization of dynamic microtubules (MTs). The bicistronic construct for expressing a cellular morphology marker (MARCKS-TagRFP) and the MT +TIP marker are linked by an internal ribosome entry site (IRES). The expression cassette is subcloned into the MCS of pSIN-TRE-S lentivirus transfer vector. Vector abbreviations: RSV, Rous sarcoma virus U3 sequence; 5′ LTR, 5′ long terminal repeats; TRE,

the myristoylated alanine-rich C-kinase substrate (MARCKS) protein fused to TagRFP-T (De Paola, Arber, & Caroni, 2003). The construct contains a myristoylation (N-terminal glycine) and palmitoylation site (introduced cysteine at position 3), which localizes TagRFP-T partially at cellular membranes and in the cytosol. The membrane association facilitates resolving of fine subcellular structures.

1.2.2 MT +TIP markers

We use GFP-MT+TIP, which contains the general MT tip localization signal, the SxIP motif and is recognized by endogenous MT plus-end binding (EB) proteins. The construct consists of a two-stranded leucine zipper coiled-coil sequence corresponding to GCN4-p1 (RMKQLEDKVEELLSKNYHLENEVARLKKLVGER) that was fused to N-terminal 18 amino acid peptide (GSRPSTAKPSKIPTPQRK) of human MACF2 (E5455-R5497; NP_899236) by PCR-based strategy (Honnappa et al., 2009). A glycine rich-linker sequence (GAGG) was inserted between GCN4-pl and MACF18. GFP is targeted N-terminal to this construct connected by a 13 amino acid linker sequence.

1.2.3 Insertion of the IRES construct into the pSIN-TRE-S lentivirus transfer vector

The bicistronic construct was generated in the pIRES vector (Clontech), which contains an attenuated IRES of the encephalomyocarditis virus. MARCKS-TagRFP-T was inserted upstream of the IRES site (NheI and MluI sites) and the GFP-MT+TIP marker downstream (XbaI and NotI sites) by a PCR-based strategy. We subcloned this expression cassette into the MCS of pSIN-TRE-S transfer vector using NheI and EcoRV restriction sites (Figure 1(A)).

tetracycline response element; MCS, multiple cloning site; Syn-Pro, 0.5 kb Synapsin promoter; rtTA2-M2, Tet-On transactivator; WPRE, Woodchuck Hepatitis Virus Posttranscriptional Regulatory Element; 3′ LTR, 3′ long terminal repeats; f1 Origin, Phage F1 origin of replication; AmpR, Ampicilin resistance; Origin of R, bacterial origin of replication. (B) Lentivirus production in HEK 293T cells. Transfer vector, packaging and envelope plasmids are transfected. Virus components are produced and assembled within the cells and infectious particles are released to the cell supernatant. Virus is concentrated from the cell supernatant by tangential flow filtration. (C) Preparation of organotypic hippocampal slice cultures. The hippocampus is dissected from both cortical hemispheres and subsequently chopped in slices of 350 μm. Slices are put on small patches of FHLC membranes, which are placed on Milicell inserts at the interface of culture medium and atmosphere. Cultures are infected by application of a drop of concentrated lentivirus. (D) Live imaging of transduced organotypic cultures. The membrane patch containing the slice culture is placed upside down in the Ludin chamber and held in position by a small metal ring. Constant perfusion with ACSF ensures sufficient oxygenation of the culture during imaging. Time-lapse recordings can be corrected for *xy* drifts and background signals, which simplify the following data analysis. (See color plate)

1.3 VIRUS PRODUCTION

- Expand HEK 293T cells (passage number <25) in complete culture medium. The final virus production is performed in a 500-cm^2 dish that is about 60–70% confluent.
- HEK 293T cells are transfected with a mixture of DNA and polyethylenimine. Prepare 35 μg p.MDG2 (addgene #12259), 65 μg psPAX (addgene #12260), and 100 μg pSIN-TRE-S transfer vector in 5 mL OptiMEM. In a second tube, add 600 μl MAXPEI stock to 5 mL OptiMEM and incubate for 5 min before combining with the DNA solution. Incubate DNA/MAXPEI mix for 20 min and then apply to cells (from now on classified biosafety level II).
- Exchange medium to 100 mL virus production medium, 6 h posttransfection. Depending on the cell density, it is advisable to buffer the culture medium by addition of HEPES. Usually, we add 2 mL HEPES after 24 h.
- Harvest virus-containing cell supernatant 48 h posttransfection. Remove debris by centrifugation (500 g for 15 min) and load 15 mL supernatant on an Amicon Ultra spin filter tube. Concentrate all virus supernatant by successive rounds of centrifugation (4000 g) and removal of flow through. The time required for sample concentration increases with each round of centrifugation (start with 5 min).
- Reduce the concentrated virus solution to ~250 μL during the last centrifugation step. Mix with equal amounts of PBS and aliquot virus in several screw cap tubes. Snap freeze virus in liquid nitrogen and store at −80 °C. Virus is stable for a minimum of 1 year but each round of thawing and freezing reduces the virus quality.
- It is recommended to test each batch of produced viruses on dissociated hippocampal neurons before infecting slice cultures. Routinely, we apply 1 μL virus to cultured DIV14–21 neurons. Protein expression is induced 3 days after infection by addition of doxycycline (500 ng/mL) and neurons are fixed 2 days later. An average virus preparation should infect at least 50 neurons on an 18-mm coverslip of a high-density culture. Additionally, it can be assessed if the virus possesses a tropism in favor of infecting astrocytes over neurons.

2. PREPARING ORGANOTYPIC SLICE CULTURES

One of the major challenges in culturing brain tissue is to supply explants with nutrition while maintaining sufficient oxygenation. Two culturing techniques have been established that results in organotypic slice cultures with slightly different properties. First, roller-tube cultures are embedded in a plasma clot on a glass coverslip (Gahwiler, 1981). The coverslips are positioned in culture tubes containing little culture medium and continuously rotated in a roller drum. The slow rotation assures an alternating contact with the culture medium and gas phase. Second, interface-type cultures are grown on semiporous membranes which are positioned at the interface

between culture medium and atmosphere (Stoppini, Buchs, & Muller, 1991). The slice remains in contact with the medium by a thin film of liquid that covers the slice and prevents drying out of the culture while still allowing gas exchange via diffusion. Both types of cultures survive for several weeks to months in vitro and retain many architectural features of the original tissue. The main difference between the two culture techniques is an increased flatting of the roller-tube cultures which give them a quasi-monolayer appearance (Gahwiler, Capogna, Debanne, McKinney, & Thompson, 1997). In comparison, interface cultures shrink less and remain organized in several layers of cells. Although, the thinning of the roller-tube cultures is advantageous for microscopy, we prefer using the interface method because cultures are easier to prepare, require less equipment, and produce more consistent results in our hands.

There are only minor differences in morphological and neurochemical properties between mature organotypic cultures and acute tissue preparations. Cutting the hippocampus in transversal orientation preserves the connectivity within the trisynaptic circuit but destroys extrinsic fibers. The resulting neuronal injury and loss of connectivity induces axonal and dendritic remodeling that occurs mostly within the first week in culture. Morphological changes that can be observed during slice culturing are a slightly higher dendritic complexity (De Simoni et al., 2003), the collateral sprouting of mossy fibers (Caeser & Aertsen, 1991; Coltman, Earley, Shahar, Dudek, & Ide, 1995), and an initial reduction in synaptic number which, however, is equalized by synaptogenesis after cultures reached maturity (De Simoni et al., 2003). Organotypic cultures express synaptic receptors and other neuronal markers (e.g., synaptophysin, MAP-2, and GAP-43) comparable to tissue of a similar developmental stage (Pena, 2010). Electrophysiological recordings of synaptic transmission appear to be normal and several forms of short- and long-term synaptic plasticity can be induced and studied in an intact synaptic network (Gahwiler et al., 1997).

In the following section, we will describe how we culture organotypic interface slice cultures and transduce these with lentivirus. We perform high resolution imaging of MT dynamics at an inverted microscope, which requires the transfer of the culture into a separate imaging chamber. Because cultures tightly adhere to the membrane after several days, we do not place them directly on the culture insert but plate each slice on an additional membrane patch, often referred to as "confetti" (Gahwiler, Thompson, & Muller, 2001). These can be easily relocated with tweezers and reduce the risk of damaging the culture.

2.1 BUFFERS, SOLUTIONS, AND EQUIPMENT

- C57BL/6 mouse pups (P5-P7) (rat pups of the same age can be also used).
- Dissection microscope in a laminar flow hood.
- Dissection tools: scalpel, angled scissors, spatulas, fine forceps.
- McIlwain tissue chopper.
- 250-µm thick PVC foil (Antalis, #453117). Cut in small pieces about the size of the McIlwain Teflon stage.

- Modified Gey's balanced salt solution (GBSS): 1.5 mM $CaCl_2$, 0.2 mM KH_2PO_4, 0.3 mM $MgSO_4$, 5 mM KCl, 1 mM $MgCl_2$, 137 mM NaCl, 0.85 mM Na_2HPO_4, 12.5 mM HEPES. Sterile GBSS can be stored for several weeks at 4 °C. Just prior dissections supplement 100 mL GBSS with 1 mL of 50% D-glucose (w/v) and 1 mL of 100 mM kynurenic acid (Sigma, K3375). Adjust pH to 7.2 and the osmolarity to 310−320 mOsm using sucrose.
- Culturing medium (100 mL): 47.75 mL MEM (Gibco, 21575-22), 25 mL HBSS (Gibco, 24020-091), 25 mL horse serum (Gibco, 16050-122), 1.25 mL HEPES (1M), and 1 mL D-glucose (3M). Adjust pH to 7.2, osmolality to 310−320 mOsm, filter, sterilize, and store at 4 °C.
- Cut small membrane patches of FHLC membrane (Millipore, FHLC01300) and sterilize in 70% EtOH for 1 h. Membrane patches are tried in sterile plastic dishes before use.
- Millicell culture inserts (Milipore, PICM0RG50).

2.2 HIPPOCAMPAL DISSECTION AND SLICE PREPARATION

- All dissecting instruments and buffers are sterilized in either 70% ethanol or by passing through a 0.22-μm filter, respectively. Standard cell culture techniques should be applied during dissection and maintenance of the cultures to avoid contaminations. All dissection steps are applied in a laminar flow hood, except for the initial decapitation and brain removal.
- Add 1 mL of culturing medium to each well of a 6-well plate. Place Millicell culture inserts and position three FHLC membrane patches per insert (avoid overlapping of the membranes). Keep plates in the incubator until slices are ready to plate.
- Decapitate animal and remove skin from the skull with a scalpel. Insert angled scissors in the foramen magnum and open the skull by cutting along the midline towards the frontal lopes. Remove the soft skull pieces with forceps. Move a rounded spatula under the brain to lift up the brain and cut optic and cranial nerves. Transfer brain into a beaker with ice-cold GBSS.
- Continue dissection in a 10-cm culture dish under the dissection microscope. We use a sterile filter paper soaked in GBSS to prevent sliding of the brain during cutting. Separate both hemispheres by cutting through the midline and remove the midbrain with a scalpel. For each hemisphere, make two transversal cuts that run in a line from the midbrain towards the cortex, flanking the outer ends of the hippocampus on both sides (a triangle-shaped piece of tissue remains). Carefully roll the hippocampus out of the cortex using a spatula. Use the spatula to cut the connection between hippocampus and cortex. We found that keeping a larger piece of cortex connected to the hippocampus increases quality and survival of mouse slice cultures.
- Place a piece of PVC foil onto the Teflon stage of the tissue chopper. Align both hippocampi perpendicular to the chopper blade and cut transversal slices of 350 μm. Transfer PVC foil carrying the chopped hippocampi into a dish

containing ice-cold GBSS. Gently shake the dish to isolate single slices and use fine forceps to separate slices still attached with each other.
- Check for slice integrity and collect undamaged slices in a dish containing cold culture medium. Use a fire-polished Pasteur pipette to transfer individual slices. Place a single slice on each FHLC membrane patch and remove excess medium with a pipette. Return the culture plates into the tissue culture incubator.

2.3 SLICE INFECTION AND MAINTENANCE OF ORGANOTYPIC CULTURES

- We usually infect slice cultures with lentivirus within 2 h after plating. Slices are transduced by direct application of a drop of 4 μL concentrated virus solution above the slice. We observed a slight increase in transduced neurons when a second drop of virus is added about 1 h after the first application.
- Virus-infected hippocampal cultures are maintained in a humidified incubator with 5% CO_2 at 37 °C (biosafety level II). Culturing medium is exchanged at DIV1 and then every 2−3 days. At DIV4−5 culture plates are moved to an incubator with identical settings except for a lowered temperature of 35 °C (now biosafety level I).

3. LIVE CELL IMAGING

Fluorescence microscopy of living neurons in tissue culture requires similar considerations as imaging of dissociated neurons in culture. For instance, similar precautions are needed to control the external milieu (temperature, pH) and to avoid cell damage (phototoxicity/bleaching). However, the three-dimensional (3D) organization of slice cultures represents an additional challenge for microscopic analysis. Axons and dendrites rarely grow in perfect vertical orientation and exhibit variable diameters that necessitate imaging of large z-stacks. Absorption and scattering of light, by overlying tissue, exponentially increase with imaging depth. This reduces the sample accessibility for single photon microscopy to a maximal depth of approximately 50 μm (Kasparov, Teschemacher, & Paton, 2002). Multiphoton microscopes, in comparison, allow a significant increase of tissue penetration depth. However, like other laser scanning systems the acquisition speed is relatively slow. In our experience, imaging of MT dynamics in slice cultures is more limited by the acquisition speed than by the need for deep tissue penetration.

3.1 BUFFERS

- ACSF: 126 mM NaCl, 3 mM KCl, 2.5 mM $CaCl_2$, 1.3 mM $MgCl_2$, 1.25 mM Na_2HPO_4, 26 mM $NaHCO_3$, 20 mM glucose, and 1 mM Trolox (Sigma, 238813), constantly oxygenated with 95% O_2, 5% CO_2.

3.2 PERFUSION SYSTEM AND IMAGING CHAMBER

The majority of slice cultures are imaged under submerged conditions. While "drowning" the slice in ACSF simplifies several experimental approaches as electrophysiological recordings and bath applications of drugs, it derogates oxygenation of the neurons within the tissue. In order to enable sufficient oxygenation, we constantly perfuse the slice with oxygenated ACSF. Our perfusion system is composed of a standard peristaltic pump (Minipuls 3, Gilson), which is connected to the ACSF reservoir and waste bottle. We installed an in-line solution heater (Warner SH-27B) in close distance to the imaging chamber in order to prevent focal drifts by temperature differences between the recording chamber and the perfused ACSF. All tubing consists of PVC which has low permeability for oxygen. At our inverted microscopes, we use the Ludin imaging chamber (Life Imaging Services, Switzerland), which features built-in perfusion inlays. The chamber is filled with ACSF prior insertion of the membrane patch bearing the slice culture. The membrane is positioned upside down onto the coverslip and is held in place by a small ring (~8 mm diameter) made of platinum. The Ludin chamber is placed into the stage incubator preheated at 37 °C and connected with the perfusion system. The complete setup is equilibrated by continuous perfusion (~300 μL/min) for at least 5 min before the start of imaging.

3.3 SPINNING DISK CONFOCAL MICROSCOPY

Imaging of MT dynamics in organotypic slice cultures require a confocal approach with very high image acquisition rates. We use a spinning disk microscope, which is substantially faster than conventional single-beam laser confocal setups. Here, the excitation laser passes a rotating disk with microlenses that create an array of laser foci on a corotating disc with holes that is positioned in a plane conjugate to the object plane. In this way, the confocal principle of a focused laser and a pinhole in a conjugate focal plane is massively parallelized and the complete field of view can be scanned within several milliseconds (Graf, Rietdorf, & Zimmermann, 2005). The Yokogawa spinning disk confocal scanning unit (CSU-X1-A1N−E) is installed on a Nikon Eclipse-Ti microscope with Plan Apo VC 100×, 1.4 NA oil objective. Samples are excited sequentially with a 491-nm laser (100 mW, Cobolt Calypso) and a 561-nm laser (100 mW, Cobolt Jive). We use the following optical filters: triple-band dichroic mirror (z405/488/568trans-pc, Chroma) in the Yokogawa unit and a fast filter wheel (CSUX1-FW-06P-01) equipped with ET-GFP (49002, Chroma) and ET-mCherry (49008, Chroma) emission filters. Images are acquired with an Evolve 512 EMCCD camera (Photometrics). The microscope is equipped with a motorized stage (ASI, PZ-2000) and a Tokai Hit stage incubator (INUG2-ZILCS-H2). The camera and all motorized parts of the microscope are controlled by MetaMorph 7.6.4 software (Molecular Devices).

3.4 LENTIVIRUS TRANSDUCTION EFFICIENCY IN ORGANOTYPIC SLICE CULTURES

Like other retroviruses, lentivirus stably integrates a copy of their genome in the host cell. Interestingly, lentivirus favors integration in active transcription units, which has potential to disrupt the host gene expression and impair viability of infected cells (Kvaratskhelia, Sharma, Larue, Serrao, & Engelman, 2014). We have tested lentiviral transduced organotypic slice cultures for signs of increased cytotoxicity but did not observe any obvious effects in this direction (Figure 2(A)). Slices preserve cytoarchitectural features of hippocampal cultures and transduced neurons show the morphological characteristics of principal cells typically for the corresponding hippocampal regions (Figure 2(B) and (D)).

Application of lentivirus, generated with the pSIN-TRE-S transfer vector, results in a sparse pattern of transduced cells in organotypic slice cultures (Figure 2(C)). This low transduction efficiency is based on an intrinsic property of the used transfer vector, as described in the first paragraph, but does not reflect the general infectious potential of lentivirus. We find the majority of infected neurons within the dentate gyrus region (Figure 2(C), red box). Neurons of the CA1 region are transduced more sporadic and CA3 neurons become hardly infected. This may be partially explained by differences in cell densities between the hippocampal regions, which influence virus accessibility during infection. Further, we noticed that different batches of produced virus differ in their potential to transduce pyramidal cells of the CA1 region. This indicates lentiviral tropism as a critical factor influencing the targeting of neuronal subpopulations in slice cultures. Apart from neurons, we generally find a varying number of transduced astrocytes that mainly localize at the edge of the culture.

4. DATA PROCESSING AND ANALYSIS WITH FIJI

Using spinning disk confocal microscopy, GFP-MT+TIP comets highlighting the growing MT plus tip can be readily imaged and followed over time in neurons of organotypic hippocampal slice cultures (Figure 3(C–F)). Manual or automatic tracking of comet trajectories can be used to analyze speeds and directionality of MT growth. In order to identify segments with high MT dynamics, we create maximum projections of entire time-lapse recordings from axonal or dendritic segments (Figure 3(C) and (D)). This results in a single image, in which each pixel value corresponds to the maximum value of that pixel position across the entire time series, respectively. Usually, the large pool of diffuse GFP-MT+TIP obscures the unambiguous identification of growing MT plus-ends. We therefore apply a set of background-reducing techniques before performing data analysis. These procedures dramatically enhance the appearance of GFP-MT+TIP comets. Kymography can be used to display comet dynamics along a line over time (Figure 3(E–J)).

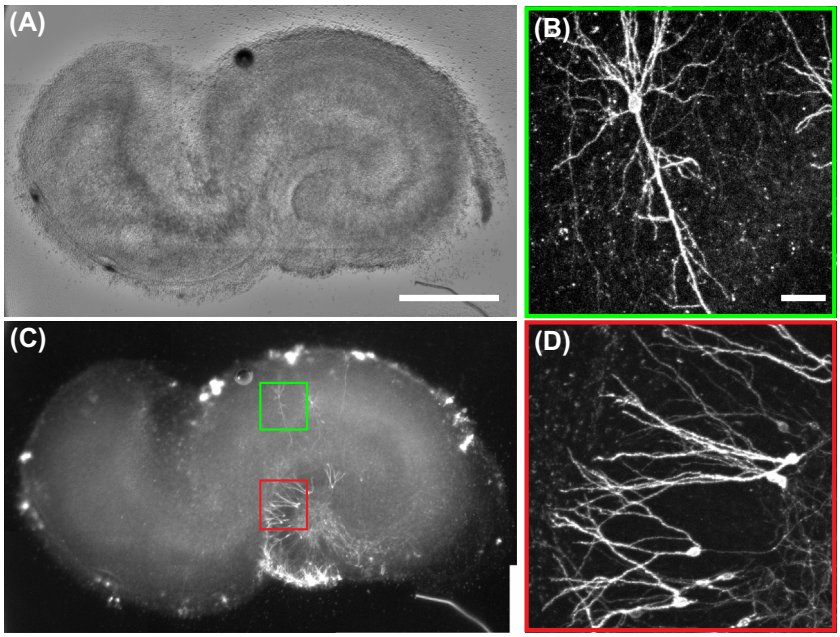

FIGURE 2 Example of transduced organotypic slice culture.

(A) Slice culture imaged via transmitted light microscopy. The picture is composed of multiple images taken with an AMG EVOS microscope using a 4× objective. Cell bodies of neurons appear as darker layers and can be clearly observed in the dentate gyrus, CA3, and CA1 region (scale bar = 1 mm). (B) CA1 pyramidal neuron of the CA1 region. Cell body, the basal dendritic tree, and the proximal part of the apical dendrite are visible. The neuron represents a maximum intensity projection of a z-stack covering the complete neuron. The MARCKS-TagRFP signal was recorded with a spinning disk confocal microscope using a 10× objective (scale bar = 50 μm). (C) Fluorescent signal of the morphology marker channel (identical slice as in (A)). Lentiviral transduced neurons localize primarily to the dentate gyrus region and less frequently to the CA1 region. Axonal trajectories (Mossy fibers) projecting from the granule cells to the CA3 region are visible as a diffuse band. The very bright signals at the edge of the culture result from infected astrocytes. (D) Granule cells of the dentate gyrus. The dendrites project in one direction while the axons point in the opposite direction. Imaging conditions are identical to (B).

4.1 IMAGE PROCESSING

- Imaging of MT dynamics in slice cultures generates a large four-dimensional dataset (*xyzt*). Analyzing this dataset in all dimensions poses a significant challenge for computer hardware and software. If the information in z is not essential for answering the experimental question, we reduce this dimension by generating average or maximum intensity projections along z axis.

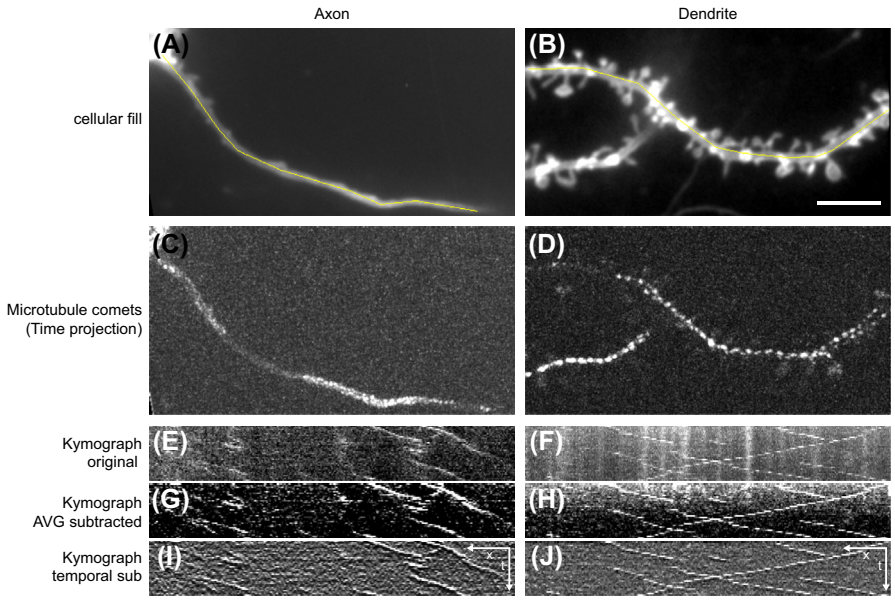

FIGURE 3 Microtubule (MT) dynamics in slice cultures.

(A and B) MARCKS-TagRFP signal (morphology marker) of a granule cell axon (A) and dendrite (B) recorded in a hippocampal slice culture. The thin line marks the region that was used to create the kymographs. Scale bar represents 5 μm. (C and D) MT plus-end movements are plotted over time (3 min) for the axon (C) and dendrite (D). Background signals were reduced in the time-lapse recordings prior projection by the running average subtraction method. (E–J) Kymographs of MT dynamics in the axon (E/G/I) and dendrite (F/H/J). The line shown in (A) and (B) was copied into the GFP-MT+TIP time-lapse stacks and was widened to 12 pixels. The FIJI plugin "KymoResliceWide" was applied with the maximum intensity setting. (E and F) Kymographs of the unprocessed data show a low signal-to-noise ratio. Additionally, stationary background signals can generate vertical lines (more evident for the dendrite example). (G and H) Images were processed with standard average subtraction and low-pass filtering before generation of the kymographs. This increases signal-to-noise ratios and reduces undesired traces in the kymographs but does not account for dynamic changes of the signal intensities. The reduction in signal intensity due to photobleaching is clearly observable along the time axis of the kymograph. (I and J) Original images were processed with a running average subtraction (two frames averaged) and low-pass filtering prior kymograph generation. Unlike average subtraction, this method also adapts to dynamic changes of the signals.

- Long-term image acquisition is often accompanied by the microscope's stage drift in *xy* directions. We use the FIJI plugin "MultiStackReg v1.45" (written by Brad Busse) on the recordings of cellular morphology to correct for the observed drift. The time shift of coordinates derived from this correction is applied to the MT marker channel (GFP-MT+TIP).

- The usage of GFP-MT+TIP as a MT plus-end marker generates significant cytosolic background signals that vary between neurons depending on the overall expression levels of the protein. We use two techniques of background subtraction on the time series, called here "standard average subtraction" and "running average subtraction." One of them is applied to the dataset dependent on the quality and nature of the recorded time-lapse (Figure 3(G–J)).

4.1.1 Standard average subtraction

First, an average projection of the whole time-lapse recording is generated. The average intensity image is then subtracted from each frame of the time-lapse recording. This method requires little computational power and is easy to apply. However, it is less efficient in the background suppression when the overall signal gradually decreases due to photobleaching or when large-area changes of the imaged structure occur, for instance, growth cone collapse or spine retraction.

4.1.2 Running average subtraction

This image-processing algorithm for each frame subtracts the average intensity projection image made from a subset of frames before the current one. The sensitivity can be varied by changing its so-called "window size," i.e., the number of frames in the subset. This method produces better results under conditions of high bleaching or when the imaged structure is motile. A drawback of this method is the loss of a few frames within the recorded time-lapse. Further, it is essential to choose sufficiently large window size to avoid overlapping of the comet signals.

- Finally, a low-pass filter is used to smooth remaining noise. Usually, we apply the "Convolve" function in FIJI with a 3 × 3 Gauss kernel (1 2 1/2 4 2/1 2 1).

4.2 ANALYZING MT DYNAMICS WITH KYMOGRAPHS

Kymographs are simple methods to represent the dynamics of moving structures in a two-dimensional (2D) figure. They allow a direct read-out of speed, direction, and intensity of the analyzed structures. In neurons, kymographs are often used to visualize vesicular trafficking along neurites and can be applied in the same way to demonstrate MT dynamics. Kymographs from time-lapse recordings can be easily generated in FIJI by drawing a line ("segmented line" tool) over the neurite of interest (Figure 3(A) and (B)). The line width is adjusted to cover the complete structure before we apply the "KymoResliceWide" plugin (written by Eugene Katrukha). As a result, we get a 2D kymograph image, where the vertical axis represents time, while the horizontal axis corresponds to the pixel's intensities along the length of the selected line (Figure 3(E) and (F)). Static and moving objects appear differently on the kymographs. Static objects appear as vertical lines parallel to the time axis, while moving ones appear as easily recognizable tilted lines (Figure 3(F)). The direction of the tilt separates objects moving in opposite directions. The filtering steps described above removes most static objects (compare Figure 3(F) and (J)). We consider this as an advantage, since we examine MTs dynamics using +TIP markers, which should

exclusively accumulate on moving (i.e., growing) MTs tips. The difference between two filtering techniques is best illustrated on Figures 3(H) and (J). The gradual background photobleaching manifesting itself as a vertical (time) intensity gradient that Figure 3(H) disappears when using the running average subtraction filtering (Figure 3(J)). In agreement with studies on dissociated neurons (Jaworski et al., 2009; Stepanova et al., 2003), we observed a bidirectional orientation of dendritic MTs, while axonal MTs extend unidirectional with the growing plus tip outwards.

CONCLUSION

Here, we presented a method to image and analyze MT dynamics in neurons of organotypic hippocampal slice cultures. This method allows imaging of axons and dendrites at high temporal and spatial resolution using spinning disk confocal microscopy. The neurites are embedded in 3D organized tissue that closely resembles the conditions found in vivo. A major challenge in applying organotypic slice cultures to fluorescent imaging is the achievement of sufficient expression of marker proteins. Ballistic transfection, viral transduction, or more recently single cell electroporation have been successfully applied. While the first approach suffers from general low efficiency, the latter requires special equipment and experience in electrophysiology. Here, we show that application of lentiviruses with an inducible expression system results in transduced neurons with high expression levels, in a sparse pattern throughout the slice culture, which is optimal for high-resolution imaging. In principle, this method could be applied to other neuronal tissue culture systems, such as cerebral organoids (Lancaster et al., 2013) or 3D Matrigel cultures (Choi et al., 2014). In addition, this method is not restricted to neuronal tissue and maybe used for visualizing MT dynamics in other mammalian 3D culture systems (Shamir & Ewald, 2014).

ACKNOWLEDGMENTS

We would like to thank Eugene Katrukha for writing several ImageJ plugins described in this chapter and for very helpful comments on the manuscript. This work was supported by the Netherlands Organization for Scientific Research (NWO-VIDI, LCK, NWO-VICI, CCH), the Netherlands Organization for Health Research and Development (ZonMW-TOP, C.C.H.), the Marie-Curie Intra-European Fellowship (MC-IEF, PS), the Human Frontier Science Program (HFSP-CDA, CCH), and by a grant from the Swiss National Science Foundation (PBZHP3_147307, PS).

SUPPLEMENTARY DATA

Supplementary data related to this article can be found online at http://dx.doi.org/10.1016/bs.mcb.2015.06.006.

REFERENCES

Akhmanova, A., & Steinmetz, M. O. (2008). Tracking the ends: a dynamic protein network controls the fate of microtubule tips. *Nature Reviews Molecular Cell Biology, 9*(4), 309−322. http://dx.doi.org/10.1038/nrm2369. pii:nrm2369.

Baas, P. W., & Ahmad, F. J. (2013). Beyond taxol: microtubule-based treatment of disease and injury of the nervous system. *Brain, 136*(Pt 10), 2937−2951. http://dx.doi.org/10.1093/brain/awt153. pii:awt153.

Baas, P. W., & Lin, S. (2011). Hooks and comets: the story of microtubule polarity orientation in the neuron. *Developmental Neurobiology, 71*(6), 403−418. http://dx.doi.org/10.1002/dneu.20818.

Bradke, F., Fawcett, J. W., & Spira, M. E. (2012). Assembly of a new growth cone after axotomy: the precursor to axon regeneration. *Nature Reviews Neuroscience, 13*(3), 183−193. http://dx.doi.org/10.1038/nrn3176. pii:nrn3176.

Breuss, M., & Keays, D. A. (2014). Microtubules and neurodevelopmental disease: the movers and the makers. *Advances in Experimental Medicine and Biology, 800*, 75−96. http://dx.doi.org/10.1007/978-94-007-7687-6_5.

Caeser, M., & Aertsen, A. (1991). Morphological organization of rat hippocampal slice cultures. *Journal of Comparative Neurology, 307*(1), 87−106. http://dx.doi.org/10.1002/cne.903070109.

Chisholm, A. D. (2013). Cytoskeletal dynamics in *Caenorhabditis elegans* axon regeneration. *Annual Review of Cell and Developmental Biology, 29*, 271−297. http://dx.doi.org/10.1146/annurev-cellbio-101512-122311.

Choi, S. H., Kim, Y. H., Hebisch, M., Sliwinski, C., Lee, S., D'Avanzo, C., et al. (2014). A three-dimensional human neural cell culture model of Alzheimer's disease. *Nature, 515*(7526), 274−278. http://dx.doi.org/10.1038/nature13800. pii:nature13800.

Coltman, B. W., Earley, E. M., Shahar, A., Dudek, F. E., & Ide, C. F. (1995). Factors influencing mossy fiber collateral sprouting in organotypic slice cultures of neonatal mouse hippocampus. *Journal of Comparative Neurology, 362*(2), 209−222. http://dx.doi.org/10.1002/cne.903620205.

Conde, C., & Caceres, A. (2009). Microtubule assembly, organization and dynamics in axons and dendrites. *Nature Reviews Neuroscience, 10*(5), 319−332. http://dx.doi.org/10.1038/nrn2631. pii:nrn2631.

De Paola, V., Arber, S., & Caroni, P. (2003). AMPA receptors regulate dynamic equilibrium of presynaptic terminals in mature hippocampal networks. *Nature Neuroscience, 6*(5), 491−500. http://dx.doi.org/10.1038/nn1046. pii:nn1046.

De Simoni, A., Griesinger, C. B., & Edwards, F. A. (2003). Development of rat CA1 neurones in acute versus organotypic slices: role of experience in synaptic morphology and activity. *Journal of Physiology, 550*(Pt 1), 135−147. http://dx.doi.org/10.1113/jphysiol.2003.039099. pii:jphysiol.2003.039099.

Dittgen, T., Nimmerjahn, A., Komai, S., Licznerski, P., Waters, J., Margrie, T. W., et al. (2004). Lentivirus-based genetic manipulations of cortical neurons and their optical and electrophysiological monitoring in vivo. *Proceedings of the National Academy of Sciences of the United States of America, 101*(52), 18206−18211. http://dx.doi.org/10.1073/pnas.0407976101. pii:0407976101.

Ehrengruber, M. U., Hennou, S., Bueler, H., Naim, H. Y., Deglon, N., & Lundstrom, K. (2001). Gene transfer into neurons from hippocampal slices: comparison of recombinant

Semliki Forest Virus, adenovirus, adeno-associated virus, lentivirus, and measles virus. *Molecular and Cellular Neurosciences, 17*(5), 855–871. http://dx.doi.org/10.1006/mcne.2001.0982. pii:S1044-7431(01)90982-0.

Encalada, S. E., & Goldstein, L. S. (2014). Biophysical challenges to axonal transport: motor-cargo deficiencies and neurodegeneration. *Annual Review of Biophysics, 43*, 141–169. http://dx.doi.org/10.1146/annurev-biophys-051013-022746.

Gahwiler, B. H. (1981). Organotypic monolayer cultures of nervous tissue. *Journal of Neuroscience Methods, 4*(4), 329–342.

Gahwiler, B. H., Capogna, M., Debanne, D., McKinney, R. A., & Thompson, S. M. (1997). Organotypic slice cultures: a technique has come of age. *Trends in Neuroscience, 20*(10), 471–477. pii:S0166-2236(97)01122-3.

Gahwiler, B. H., Thompson, S. M., & Muller, D. (2001). Preparation and maintenance of organotypic slice cultures of CNS tissue. *Current Protocols in Neuroscience*, (Chapter 6), Unit 6.11. http://dx.doi.org/10.1002/0471142301.ns0611s09.

Graf, R., Rietdorf, J., & Zimmermann, T. (2005). Live cell spinning disk microscopy. *Advances in Biochemical Engineering/Biotechnology, 95*, 57–75.

Hirokawa, N., Niwa, S., & Tanaka, Y. (2010). Molecular motors in neurons: transport mechanisms and roles in brain function, development, and disease. *Neuron, 68*(4), 610–638. http://dx.doi.org/10.1016/j.neuron.2010.09.039. pii:S0896-6273(10)00781-6.

Honkura, N., Matsuzaki, M., Noguchi, J., Ellis-Davies, G. C., & Kasai, H. (2008). The subspine organization of actin fibers regulates the structure and plasticity of dendritic spines. *Neuron, 57*(5), 719–729. http://dx.doi.org/10.1016/j.neuron.2008.01.013. pii:S0896-6273(08)00074-3.

Honnappa, S., Gouveia, S. M., Weisbrich, A., Damberger, F. F., Bhavesh, N. S., Jawhari, H., et al. (2009). An EB1-binding motif acts as a microtubule tip localization signal. *Cell, 138*(2), 366–376. http://dx.doi.org/10.1016/j.cell.2009.04.065. pii:S0092-8674(09)00638-2.

Hoogenraad, C. C., & Bradke, F. (2009). Control of neuronal polarity and plasticity – a renaissance for microtubules? *Trends in Cell Biology, 19*(12), 669–676. http://dx.doi.org/10.1016/j.tcb.2009.08.006. pii:S0962-8924(09)00183-4.

Jaworski, J., Kapitein, L. C., Gouveia, S. M., Dortland, B. R., Wulf, P. S., Grigoriev, I., et al. (2009). Dynamic microtubules regulate dendritic spine morphology and synaptic plasticity. *Neuron, 61*(1), 85–100. http://dx.doi.org/10.1016/j.neuron.2008.11.013. pii:S0896-6273(08)00967-7.

Kasparov, S., Teschemacher, A. G., & Paton, J. F. (2002). Dynamic confocal imaging in acute brain slices and organotypic slice cultures using a spectral confocal microscope with single photon excitation. *Experimental Physiology, 87*(6), 715–724. pii:EPH_2480.

Kumar, M., Keller, B., Makalou, N., & Sutton, R. E. (2001). Systematic determination of the packaging limit of lentiviral vectors. *Human Gene Therapy, 12*(15), 1893–1905. http://dx.doi.org/10.1089/104303401753153947.

Kvaratskhelia, M., Sharma, A., Larue, R. C., Serrao, E., & Engelman, A. (2014). Molecular mechanisms of retroviral integration site selection. *Nucleic Acids Research, 42*(16), 10209–10225. http://dx.doi.org/10.1093/nar/gku769. pii:gku769.

Lancaster, M. A., Renner, M., Martin, C. A., Wenzel, D., Bicknell, L. S., Hurles, M. E., et al. (2013). Cerebral organoids model human brain development and microcephaly. *Nature, 501*(7467), 373–379. http://dx.doi.org/10.1038/nature12517. pii:nature12517.

Maday, S., Twelvetrees, A. E., Moughamian, A. J., & Holzbaur, E. L. (2014). Axonal transport: cargo-specific mechanisms of motility and regulation. *Neuron, 84*(2), 292−309. http://dx.doi.org/10.1016/j.neuron.2014.10.019. pii:S0896-6273(14)00917-9.

Millecamps, S., & Julien, J. P. (2013). Axonal transport deficits and neurodegenerative diseases. *Nature Reviews Neuroscience, 14*(3), 161−176. http://dx.doi.org/10.1038/nrn3380. pii:nrn3380.

Nakagawa, T., Feliu-Mojer, M. I., Wulf, P., Lois, C., Sheng, M., & Hoogenraad, C. C. (2006). Generation of lentiviral transgenic rats expressing glutamate receptor interacting protein 1 (GRIP1) in brain, spinal cord and testis. *Journal of Neuroscience Methods, 152*(1−2), 1−9. http://dx.doi.org/10.1016/j.jneumeth.2005.08.001. pii:S0165-0270(05)00279-7.

Oh, W. C., Parajuli, L. K., & Zito, K. (2015). Heterosynaptic structural plasticity on local dendritic segments of hippocampal CA1 neurons. *Cell Reports, 10*(2), 162−169. http://dx.doi.org/10.1016/j.celrep.2014.12.016. pii:S2211-1247(14)01045-6.

Pena, F. (2010). Organotypic cultures as tool to test long-term effects of chemicals on the nervous system. *Current Medicinal Chemistry, 17*(10), 987−1001. pii:BSP/CMC/E-Pub/060.

Shamir, E. R., & Ewald, A. J. (2014). Three-dimensional organotypic culture: experimental models of mammalian biology and disease. *Nature Reviews Molecular Cell Biology, 15*(10), 647−664. http://dx.doi.org/10.1038/nrm3873. pii:nrm3873.

Stepanova, T., Slemmer, J., Hoogenraad, C. C., Lansbergen, G., Dortland, B., De Zeeuw, C. I., et al. (2003). Visualization of microtubule growth in cultured neurons via the use of EB3-GFP (end-binding protein 3-green fluorescent protein). *Journal of Neuroscience, 23*(7), 2655−2664. pii:23/7/2655.

Stoppini, L., Buchs, P. A., & Muller, D. (1991). A simple method for organotypic cultures of nervous tissue. *Journal of Neuroscience Methods, 37*(2), 173−182. pii:0165-0270(91)90128-M.

Tischfield, M. A., Cederquist, G. Y., Gupta, M. L., Jr., & Engle, E. C. (2011). Phenotypic spectrum of the tubulin-related disorders and functional implications of disease-causing mutations. *Current Opinion in Genetics and Development, 21*(3), 286−294. http://dx.doi.org/10.1016/j.gde.2011.01.003. pii:S0959-437X(11)00006-2.

Tonnesen, J., Katona, G., Rozsa, B., & Nagerl, U. V. (2014). Spine neck plasticity regulates compartmentalization of synapses. *Nature Neuroscience, 17*(5), 678−685. http://dx.doi.org/10.1038/nn.3682. pii:nn.3682.

Torashima, T., Yamada, N., Itoh, M., Yamamoto, A., & Hirai, H. (2006). Exposure of lentiviral vectors to subneutral pH shifts the tropism from Purkinje cell to Bergmann glia. *European Journal of Neuroscience, 24*(2), 371−380. http://dx.doi.org/10.1111/j.1460-9568.2006.04927.x. pii:EJN4927.

Zempel, H., & Mandelkow, E. (2014). Lost after translation: missorting of Tau protein and consequences for Alzheimer disease. *Trends in Neuroscience, 37*(12), 721−732. http://dx.doi.org/10.1016/j.tins.2014.08.004. pii:S0166-2236(14)00131-3.